Tailor-Made Peptide Inhibitors

DOI: 10.1002/anie.201309721

Harnessing the Evolvability of Tricyclic Microviridins To Dissect Protease–Inhibitor Interactions**

*Annika R. Weiz, Keishi Ishida, Felix Quitterer, Sabine Meyer, Jan-Christoph Kehr, Kristian M. Müller, Michael Groll, Christian Hertweck, and Elke Dittmann**

Abstract: *Understanding and controlling proteolysis is an important goal in therapeutic chemistry. Among the natural products specifically inhibiting proteases microviridins are particularly noteworthy. Microviridins are ribosomally produced and posttranslationally modified peptides that are processed into a unique, cagelike architecture. Here, we report a combined rational and random mutagenesis approach that provides fundamental insights into selectivity-conferring moieties of microviridins. The potent variant microviridin J was co-crystallized with trypsin, and for the first time the three-dimensional structure of microviridins was determined and the mode of inhibition revealed.*

Misregulation of proteolytic enzymes plays a major role in life-threatening diseases including cardiovascular and inflammatory diseases, cancer, and bacterial, and viral pathologies.[1] Cyanobacteria are an exceptionally rich source of natural serine protease inhibitors, including the microviridin class of compounds.[2] Microviridins possess a 12–14-membered peptide backbone featuring noncanonical lactone and lactam rings.[3] The metabolites belong to the ribosomally produced and posttranslationally modified peptides (RiPPs) that are increasingly recognized for their biotechnological potential.[4] Microviridins are biosynthesized from the ribosomal prepeptide precursor MdnA and subsequently modified through the action of three posttranslational modification enzymes (PTMs) (Figure 1 a).[5] Thereafter, the leader peptide part of the precursor is cleaved off by a yet unknown protease (Figure 1 a). Mutational studies of the core peptide region revealed a low promiscuity of the two cycle-forming ATP grasp ligases in vitro.[6] Here, we have assessed the capability of the microviridin in vivo production platform as an evolvable tool to dissect the role of individual amino acids for protease selectivity.

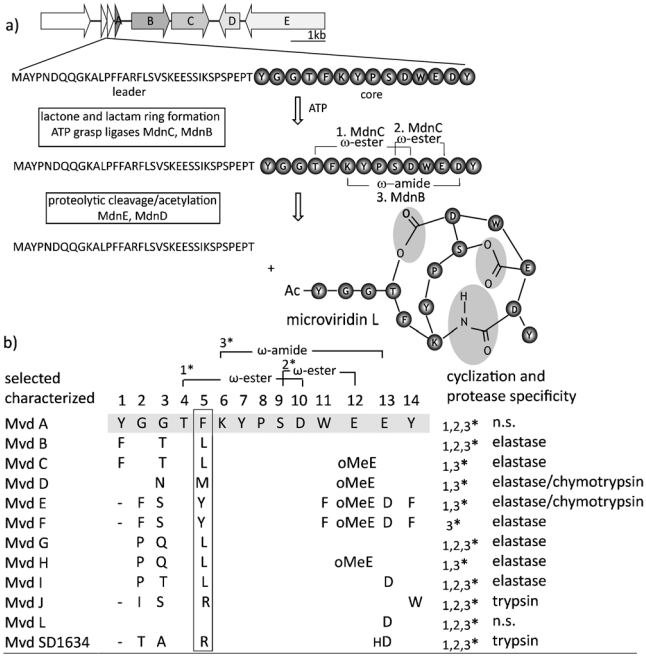

Figure 1. a) Schematic representation of microviridin biosynthesis. b) Sequence variation and protease selectivity of characterized microviridins from laboratory strains. Ac: acetylation, n.s.: no specificity, oMeE: glutamate methyl ester, HD: β-hydroxyasparatic acid.

To tailor novel microviridins we have developed a natural-diversity-guided engineering approach for microviridins based on bioactivity profiles and sequence information of characterized microviridin variants (Figure 1 b). The previously constructed minimal expression platform producing the microviridin L type was used as a template.[7] A primary focus was given to the flexible position 5 that is distinct in microviridin variants showing either elastase, trypsin, or chymotrypsin selectivity (Figure 1 b).[8] Engineered variants in *E. coli* were predominantly cleaved at position 2 of the core peptide (Figure 2). The correct cyclization and *N*-acetylation

[*] Dr. A. R. Weiz,[+] S. Meyer, Dr. J. C. Kehr, Prof. Dr. E. Dittmann
Institute of Biochemistry and Biology, University of Potsdam
Karl-Liebknecht-Strasse 24–25, 14476 Potsdam-Golm (Germany)
E-mail: editt@uni-potsdam.de
Dr. K. Ishida,[+] Prof. Dr. C. Hertweck
Leibniz Institute for Natural Product Research and Infection Biology HKI
Beutenbergstrasse 11a, 07745 Jena (Germany)
Prof. Dr. K. M. Müller
Technologie-Fakultät, Universität Bielefeld (Germany)
F. Quitterer,[+] Prof. Dr. M. Groll
Center for Integrated Protein Sciences Munich (CIPSM)
Technische Universität München
85474 Garching (Germany)
[+] These authors contributed equally to this work.

[**] We are grateful to Katrin Hinrichs for technical assistance and to Maria Poetsch and Tom Bretschneider for MALDI-TOF-MS measurements. We thank the staff of the beamline X06SA at the Paul Scherer Institute, Swiss Light Source, Villigen, Switzerland for their help with data collection. This work was supported by the German Research foundation (DFG) (Di910/4-1 to E.D.) and (He3469/4-1 to C.H.) and by a grant in the cluster of excellence UniCAT (to E.D.).
Supporting information for this article is available on the WWW under http://dx.doi.org/10.1002/anie.201309721.

of the peptides was confirmed by MALDI MS and post-source decay (PSD) analysis (Figures S1–S3 in the Supporting Information). IC_{50} values were determined for six serine-type proteases.

Remarkably, the exchange of the Phe residue in microviridin L with Leu, Met, Arg, and Tyr led to a strong increase in inhibitory activities towards elastase, subtilisin, trypsin, and chymotrypsin, respectively (Figure 2). The single amino acid exchange in the F5L variant shifted the activity towards elastase in the nanomolar range. Further stepwise point mutations of flexible positions within microviridins using a widespread microviridin field variant[9] as a template had only minor impact on the overall inhibitory activity against elastase (G2N/G3V/F5L/D13E, Figure 2). Similarly, changes at position 7 had no significant consequences. The exchange of the Trp at position 11 led to loss of production. The same phenomenon was observed when we tried to increase or decrease the size of the first ring of microviridins between Tyr and Asp (positions 4 and 10) and when we exchanged the amino acid positions forming the second ring, Ser and Glu (positions 9 and 12) (Figure 2). These results demonstrate the pivotal importance of position 5 for the bioactivity profile of microviridins. Moreover, the respective amino acids at this position in the most active variants represent perfect substrates for the specific target proteases, suggesting a substrate-like interaction of microviridins with the corresponding proteases. We have further calculated the K_i values of selected microviridin types using a tight competitive binding model (Table S5).

Subsequently, we have translated the results of our rational approach into a random mutagenesis study. Specifically, we have generated a library of microviridins focusing on the highly variable positions 1, 2, 3, 5, and 14 using randomized oligonucleotide synthesis. The yield and processing efficiency strongly differed in selected clones (Figure S4). With this approach we could eventually identify a single clone (encoding Phe and Ala at positions 1 and 2, respectively) that produced high amounts of a correctly processed tricyclic and *N*-acetylated microviridin with only low amounts of incompletely processed side products (Figure S4). As the low processing efficiency is a major bottleneck in the microviridin production platform a focused microviridin library was constructed by randomizing only the codon for the selective position 5, whilst keeping the Phe and Ala codons at the N-terminus. The library was then used to develop a colorimetric whole-cell screening assay (Figure 3) using substrates containing *p*-nitroanilide (*p*-NA) for elastase, trypsin, and subtilisin, respectively. Active clones were sequenced and the resulting peptides were purified and further characterized. The correct cyclization and *N*-acetylation of all variants was confirmed by MALDI MS and PSD analysis (Figure S1). Chymotrypsin, thrombin, and plasmin were included in the bioactivity profiling. The most potent microviridin types isolated in the elastase screening carried Leu or Val at position 5, whereas the trypsin trial yielded active variants carrying either Arg or Lys at this position. The IC_{50} values obtained for the random variants carrying Ala at position 2 (Figure 3) were slightly higher than those of the respective rational variants carrying Gly at position 2 (Figure 2), indicating an impact of the N-terminal side chain for the overall bioactivity. The subtilisin screening resulted in a number of active clones including the F5L, F5V, and F5K types (Figure 3). None of the purified microviridins showed activity against chymotrypsin or thrombin. The variant carrying Lys at position 5, however, showed activity against plasmin in the low micromolar range.

In order to interpret the engineering results for microviridins and to further rationalize the approach we aimed to get more structural insights on the interaction. Microviridin J

microviridin variants	elastase	chymo-trypsin	trypsin	subtilisin	thrombin	plasmin	yield in µg/ml
	inhibitory activity (IC_{50}) in µmol/l						
MvdL1	>64	24	>64	5.8	>64	>64	0.56
F5L	**0.13**	18	>59	3.8	>59	>59	0.24
F5M	8.1	13	>65	**0.09**	>65	>65	0.65
F5R	>32	>32	**4.5**	15.4	>64	>64	0.54
F5Y	>32	**8.3**	>64	0.55	>64	>64	0.48
G2N/G3V/F5L/D13E	0.38	>60	>60	13	>60	>60	*
Y7W	>64	20	>63	5.0	>63	>63	0.47
Y7F	>65	13	>65	5.1	>65	>65	0.34
W11C	--	--	--	--	--	--	--
W11S	n.d.	n.d.	n.d.	n.d.	n.d.	n.d.	*
S9A	>84	20	>84	n.d.	n.d.	n.d.	*
S9E/E12S	--	--	--	--	--	--	--
G3T/T4A	--	--	--	--	--	--	--
T4A/F5T	--	--	--	--	--	--	--

Figure 2. Rational mutagenesis of the microviridin core peptide. Significantly improved inhibitory activities are depicted with bold letters. For analytical confirmation see Figures S1 and S2. n.d.: not determined, *: close to detection limit, – : nomicroviridins detectable, lea.: leader peptide, oMe: glutamate methyl ester.

microviridin variants	elastase	chymo-trypsin	trypsin	subtilisin	thrombin	plasmin	yield in µg/ml
	inhibitory activity (IC_{50}) in µmol/l						
G2A/F5L	**0.65**	14	>65	**0.78**	>65	>65	0.99
G2A/F5I	5.2	>33	>65	>33	>65	>65	0.76
G2A/F5V	**0.16**	66	>66	**0.4**	>66	>66	0.56
G2A/F5K	>65	>65	**2.5**	**0.32**	>65	**2.0**	0.65
G2A/F5R	64	>64	**1.8**	**0.64**	>64	47	0.17

Figure 3. Results of colorimetric screening. Altered amino acids are shown in light gray. Significantly improved bioactivities are highlighted with bold letters.

and trypsin were selected as ligand and protease, due to the remarkable IC_{50} value (90 nM) reported for this protein–inhibitor pair (Table S6). The molecular architecture of the complex and the interaction of microviridin J with bovine trypsin were determined by co-crystallization. The complex crystallized in two different space groups at pH 6.5 (CS I, 1.35 Å, PDB ID: 4KTU) and 8.5 (CS II, 1.30 Å, PDB ID: 4KTS), for details see Table S7. The electron density map for CS II proved that the entire inhibitor molecule as well as the trypsin protease is fully defined, whereas in CS I, the Trp14 of the inhibitor (iTrp14) is structurally disordered (Figure 4, Figures S5 and S7).

The overall structure of microviridi J bound to trypsin displays conspicuous characteristics. Hereby, the N-terminus of the inhibitor is flexible: While iAc1, iIle2, and iSer3 in CS I protrude into a hydrophobic shallow pocket located on the surface of trypsin (Leu99 and Trp215), these N-terminal residues are rotated by approximately 150° along the C1–C2 bond of iSer3 in CS II and thus are not in contact with the protein (cf. Figure S5b). In contrast, in both crystal structures iThr4, iArg5, andiLys6 (P2, P1, and P1′) adopt a classical substrate-like trypsin binding motif. More specifically, the methyl group of the iThr4 side chain points towards Leu99 of the S2 pocket, whereas the iArg5 side chain is coordinated by the carboxyl group of Asp189 (2.9 Å) at the bottom of the S1 pocket. Furthermore, the aliphatic patch of the iLys6 side chain forms van der Waals contacts with the disulfide bond connecting Cys42 and Cys58 of the S1′ subsite. These interactions prearrange microviridin J to perfectly bind to trypsin, while the C-terminal part of the inhibitor, iSer9–iTrp14, captures a helical conformation. Interestingly, this helix is substantially stabilized by the intramolecular covalent linkages of microviridin J. In addition, intramolecular polar contacts, as shown in Figure S6, abolish any flexibility of the inhibitor between residues iThr4 and iGlu13.

Although the active-site nucleophile Ser195O^{γ} of the catalytic triad, comprising residues His57 and Asp102, is positioned in a perfect Bürgi–Dunitz trajectory towards the iArg5 carbonyl carbon of the inhibitor (distance: 2.5 Å), the peptide bond between amino acids 5 and 6 is unaffected and thus intact as shown in both crystal structures (Figure 4d). Hence, the compact structure and the ring strain of microviridin J caused by the intramolecular posttranslational covalent linkages of the side chains and its polar contacts counteract a cleavage of the compound.

Next, we performed ITC experiments to estimate enthalpic and entropic contributions to the binding affinity of trypsin and microviridin J. The analysis revealed that the interaction is both enthalpically and entropically driven with a K_D value of 0.68 μM (Figure S7), thus excluding ligand turnover, which is in agreement to the crystallographic results. Notably, this mode of inhibition is similar to that described for the cyanobacterial trypsin inhibitor A90720A,[10] yet the overall architectures of both natural products differ considerably (Figure S8). Furthermore and in contrast to microviridins, the diverse group of peptidic cyanopeptolins[11] including A90720A are produced by a nonribosomal peptide synthetase (NRPS) assembly line[12] and thus are not as accessible to genetic engineering as the RiPP type of peptide.

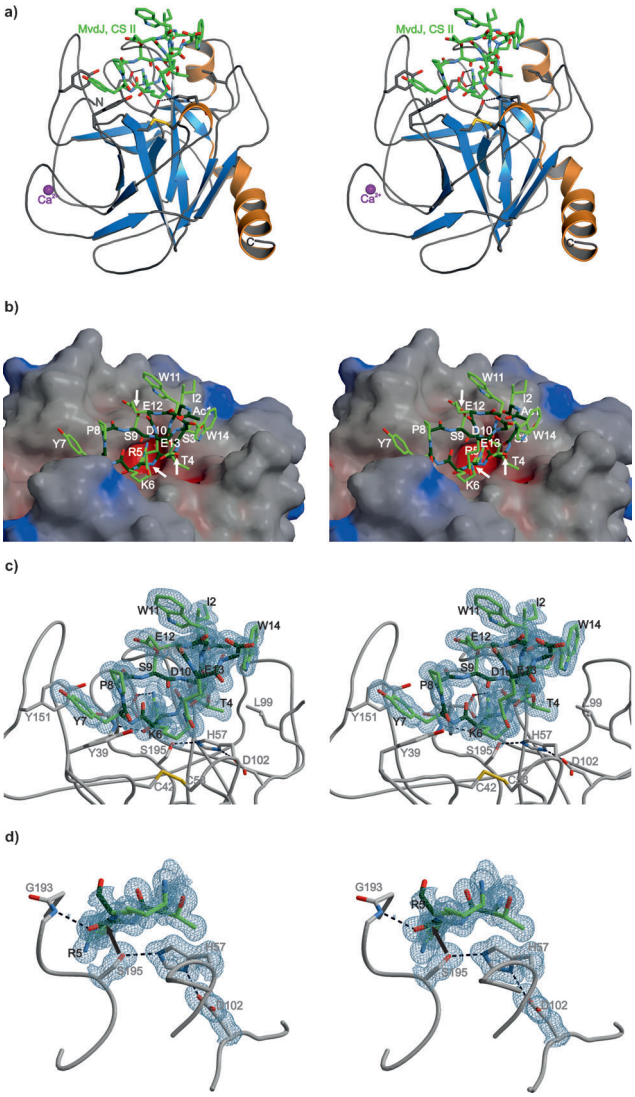

Figure 4. a) Ribbon representation of trypsin in complex with microviridin J (CS II) (green). Protein residues are shown as stick models. Ca^{2+} is shown as a purple sphere. b) Potential surface representation of trypsin in complex with microviridin J (CS II), which is shown as a ball-and-stick model. Microviridin J backbone atoms are dark green, microviridin J side chains are green. Intramolecular covalent linkages are indicated by a white arrows. c) Omit electron density map ($2F_o-F_c$) of microviridin J (CS II), contoured at 1.0σ. Interactions in the catalytic triad (His57, Asp102, and Ser195) are indicated by dashed lines. d) Omit electron density map ($2F_o-F_c$) of the catalytic triad, Gly193, which forms the oxyanion hole, and iThr4–iLys6 of microviridin J. The absence of the nucleophilic attack of Ser195 to the iArg5 carbonyl carbon is shown by a black arrow.

In summary, we have demonstrated the great potential of the microviridin engineering platform for use as a cost-effective tool for deciphering determinants underlying selectivity against different types of serine proteases. Here, we have primarily optimized the microviridin residue directly interacting with the S1 site of the enzymes, yet both mutagenesis and crystallization data indicate further potential for improving the affinity and reducing the size of the molecule.

Rational and random mutagenesis of RiPPs has proven to be a powerful avenue to generate novel biologically active

peptides, in particular lantibiotics.[13] In this study we report the first successful selective modification of a RiPP metabolite to specifically bind to different targets. Thus, our data not only reveal a great potential for therapeutic development, but may also inspire the design of peptidomimetic protease inhibitors applying synthetic chemistry.

Received: November 7, 2013
Revised: January 3, 2014
Published online: March 3, 2014

Keywords: cyanobacteria · peptide engineering · protease inhibitors · RiPPs · structure elucidation

[1] B. Turk, *Nat. Rev. Drug Discovery* **2006**, *5*, 785 – 799.
[2] M. Welker, H. von Dohren, *FEMS Microbiol. Rev.* **2006**, *30*, 530 – 563.
[3] M. O. Ishitsuka, T. Kusumi, H. Kakisawa, K. Kaya, M. M. Watanabe, *J. Am. Chem. Soc.* **1990**, *112*, 8180 – 8182.
[4] P. G. Arnison, M. J. Bibb, G. Bierbaum, A. A. Bowers, T. S. Bugni, G. Bulaj, J. A. Camarero, D. J. Campopiano, G. L. Challis, J. Clardy et al., *Nat. Prod. Rep.* **2013**, *30*, 108 – 160.
[5] a) B. Philmus, G. Christiansen, W. Y. Yoshida, T. K. Hemscheidt, *ChembioChem* **2008**, *9*, 3066 – 3073; b) N. Ziemert, K. Ishida, A. Liaimer, C. Hertweck, E. Dittmann, *Angew. Chem.* **2008**, *120*, 7870 – 7873; *Angew. Chem. Int. Ed.* **2008**, *47*, 7756 – 7759.
[6] B. Philmus, J. P. Guerrette, T. K. Hemscheidt, *ACS Chem. Biol.* **2009**, *4*, 429 – 434.
[7] A. R. Weiz, K. Ishida, K. Makower, N. Ziemert, C. Hertweck, E. Dittmann, *Chem. Biol.* **2011**, *18*, 1413 – 1421.
[8] a) M. Murakami, Q. Sun, K. Ishida, H. Matsuda, T. Okino, K. Yamaguchi, *Phytochemistry* **1997**, *45*, 1197 – 1202; b) T. Okino, H. Matsuda, M. Murakami, K. Yamaguchi, *Tetrahedron* **1995**, *51*, 10679 – 10686; c) T. Rohrlack, K. Christoffersen, M. Kaebernick, B. A. Neilan, *Appl. Environ. Microbiol.* **2004**, *70*, 5047 – 5050; d) H. J. Shin, M. Murakami, H. Matsuda, K. Yamaguchi, *Tetrahedron* **1996**, *52*, 8159 – 8168.
[9] N. Ziemert, K. Ishida, A. Weiz, C. Hertweck, E. Dittmann, *Appl. Environ. Microbiol.* **2010**, *76*, 3568 – 3574.
[10] A. Y. Lee, T. A. Smitka, R. Bonjouklian, J. Clardy, *Chem. Biol.* **1994**, *1*, 113 – 117.
[11] a) C. Martin, L. Oberer, T. Ino, W. A. König, M. Busch, J. Weckesser, *J. Antibiot.* **1993**, *46*, 1550 – 1556; b) U. Matern, C. Schleberger, S. Jelakovic, J. Weckesser, G. E. Schulz, *Chem. Biol.* **2003**, *10*, 997 – 1001; c) L. A. Salvador, K. Taori, J. S. Biggs, J. Jakoncic, D. A. Ostrov, V. J. Paul, H. Luesch, *J. Med. Chem.* **2013**, *56*, 1276 – 1290.
[12] T. B. Rounge, T. Rohrlack, A. Tooming-Klunderud, T. Kristensen, K. S. Jakobsen, *Appl. Environ. Microbiol.* **2007**, *73*, 7322 – 7330.
[13] P. J. Knerr, W. A. van der Donk, *Annu. Rev. Biochem.* **2012**, *81*, 479.

